

Supporting Information for

**Photosynthetic H₂ Generation and Organic Transformations
with CdSe@CdS-Pt Nanorods for Highly Efficient Solar-to-
Chemical Energy Conversion**

Agosti Amedeo¹, Yifat Nakibli², Amirav Lilac^{2}, Bergamini Giacomo^{1*}*

¹*Chemistry Department “Giacomo Ciamician”, University of Bologna, 40129 Bologna, Italy*

²*Schulich Faculty of Chemistry, Technion-Israel Institute of Technology, 32000 Haifa, Israel*

*Corresponding Authors' e-mail addresses:

Lilac Amirav: lilac@technion.ac.il; Giacomo Bergamini: giacomo.bergamini@unibo.it

1 PHOTOCATALYST SYNTHESIS

1.1 Synthesis of Cadmium Selenide Quantum Dots (CdSe QDs):

CdSe Seeds were synthesized following Carbone, Manna L. and co-authors procedure[1]. 60mg of Cadmium Oxide (CdO) 0.280g of Octadecylphosphonic acid (ODPA) and 3.0g of Trioctylphosphine oxide (TOPO) are heated to 150°C in a 25mL three-neck flask flushed under argon, followed by a 1 hour long vacuum stage. Then, again under argon, the solution is heated to 300°C. At this point, 1.5 g of Trioctylphosphine (TOP) is injected into the flask. The temperature is raised to 370°C and the solution is removed from the heating mantle. Upon cooling, at 350-330°C, TOP:Se solution (0.058g Se + 0.360gTOP) is rapidly injected. The reaction time is modified in order to synthesize CdSe dots of different sizes. In this work we used 2.3 nm CdSe seeds with green fluorescent, obtained by removal of the heating mantle immediately after the injection. After the synthesis, the nanocrystals are precipitated with methanol, and are washed by repeated redissolution in toluene and precipitation with the addition of methanol.

1.2 Synthesis of Cadmium Sulfide Seeded Rods (CdSe@CdS):

The procedure for the seeded rods synthesis was adopted from Talapin, Alivisatos et al.[2]. 0.230 g of CdO, 1.08 g of ODPA, 0.075g of Propylphosphonic acid, and 3.35 g of TOPO were loaded into a 25 mL three-neck flask and heated to 120°C for 30 min under vacuum. The mixture was heated to 320 °C under flowing argon to produce an optically clear solution. After the CdO completely dissolved, the solution was cooled to 120°C and put under vacuum for 2 h for removal of water, after which it was heated to 340°C under flowing Ar. At this time, 1.5 g of TOP was injected and the flask was allowed to return to 340°C. TOP:S was prepared by reacting equimolar amounts of TOP and elemental sulfur under inert atmosphere. 0.65 g TOP:S was injected into the flask at 340 °C, followed after 20 s by the injection of the CdSe seeds dissolved in 0.50 g of TOP. The CdSe solution was prepared by evaporating 0.3 g of $5 \cdot 10^{-3}$ M solution of CdSe nanocrystals in toluene and redispersing in TOP (gentle sonication might be necessary). The reaction temperature was adjusted to 320 °C, and the reaction was stopped after 15 min by the removal of the heating mantle and the injection of 4 mL of anhydrous toluene. The nanorods were isolated and cleaned by a few repeatable steps of precipitation and redissolution using toluene/hexane/chloroform as solvent and isopropanol/methanol as nonsolvent (10:7 solvent to nonsolvent ratio), with the alternating addition octalamine and nonanoic acid (about 1-2 ml). Precipitation was achieved by centrifugation for 20-30 min under 4000 rpm. Modifications to this synthetic procedure allow for control of nanorod

length and diameter. The length of the rods could be controlled by the injection of different amounts of CdSe dots with more dots producing shorter rods. Also, the reaction time could be changed to control rod length; longer growth times produce longer rods. Finally, the diameter and length of the rods could be controlled by the amount of TOP:S injected into the reaction; more TOP:S produces longer and skinnier rods.

1.3 Colloidal Growth of Platinum Metal Tips on CdSe@CdS Nanorods:

The procedure for colloidal Pt tipping was adopted from Mokari T. and coauthors[3]. Oleic acid (0.2 mL), oleylamine (0.2 mL), 43.0 mg of 1,2-hexadecanediol and 10 ml of diphenyl ether were loaded into a 25 mL three-neck flask and heated to 80 °C under vacuum for 30 min to remove traces of water. Pt acetylacetonate (13 mg) was added to a suspension of CdSe@CdS rods (about half of the synthesis product (~ 16.4 mg) in dichlorobenzene (DCB, ~1 ml) and the solution was sonicated for a few seconds to promote dissolution of the Pt precursor. Under argon, the mixture of surfactants and diphenyl ether was heated to 200 °C. At this point the Pt precursor and seeded rods in dichlorobenzene were injecting into the flask. Upon temperature recovery to 200 °C the solution turned black. After several minutes (about 4 min; the time depends on the amount of seeded rods and the quality of their cleaning procedure) the reaction was removed from the heating mantle and quenched in a water bath. The Pt tipped nanorods were isolated and cleaned by a few repeatable steps of precipitation/redissolution. Homogenous nucleation of Pt dots in the reaction flask contributed to the strong black colure of the crude product. The clean solution of Pt tipped seeded rods in toluene is brown. The key factor determining the amount of tips that will grow on each rod is the Pt-NR molar ratio.

1.4 Ligand Exchange:

The TOP ligands on the tipped seeded rods with 11-mercaptoundecanoic acid (MUA), a polar ligand that will allow the particles to be well dispersed and suspended in water. The platinum tipped seeded rods are precipitated from solution (via the addition of non-solvent and the use of centrifuge). Next, 250 mg of 11- mercaptoundecanoic acid are dissolved in 20g of methanol. Tetramethylammonium hydroxidepentahydrate salt is added until solution pH of 11 is obtained. The MUA solution in methanol is added to the particles residue and. This should result in a clean brown solution. Next, the particles are precipitated from the methanol using toluene as non solvent and centrifuging at 6000 rpm. The particles are then redispersed in water.

2 OPTICAL CHARACTERIZATION

2.1 UV/Vis Absorption Spectra

UV/Vis absorption spectra were recorded with a PerkinElmer 140 spectrophotometer, using quartz cells with path length of 1.0 cm. Fluorescence spectra were obtained with a PerkinElmer LS-50 spectrofluorimeter, equipped with a Hamamatsu R928 phototube. Spectra were used frequently to determine seed size, seed concentration, rod concentration, and the absorbance (Abs) of solutions used for hydrogen production (in addition to applications that are described in the main text).

2.2 Fluorescence Quantum Yield.

Fluorescence spectra were obtained with a PerkinElmer LS-50 spectrofluorimeter, equipped with a Hamamatsu R928 phototube. Fluorescence quantum yields were measured following the method of Resch-Genger et al.[4] The estimated experimental errors are: 2 nm on the band maximum, 5% on the molar absorption coefficient and log K values, 10% on the fluorescence quantum yield.

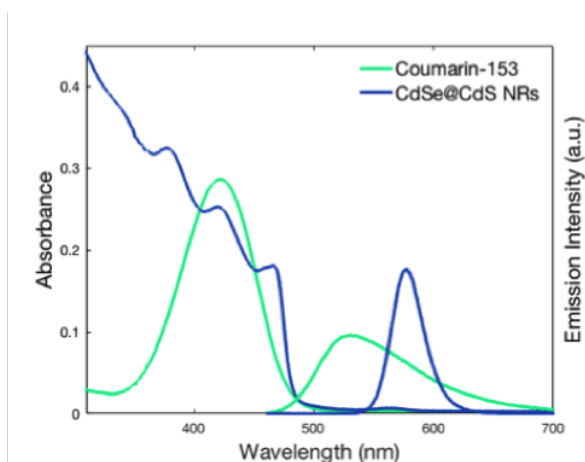


Figure S1. Relative fluorescence quantum yield (Φ_f) of CdSe@CdS NRs in toluene, using Coumarin-153 ($\Phi_f = 0.53$) as standard. Measurement and calculations were performed according to the protocol proposed by Resch-Genger et al.[4].

$$\Phi_{f,NRs}(\lambda_{exc} = 450nm) = 0.4$$

2.3 Fluorescence Lifetime

Fluorescence lifetime measurements were performed by an Edinburgh FLS920 spectrofluorimeter equipped with a TCC900 card for data acquisition in time-correlated single-photon counting experiments (0.5 ns time resolution) with a D2 lamp and a LDH-P-C-405 pulsed diode laser.

3 STERN-VOLMER ANALYSIS

Stern-Volmer analysis of the bare NRs / quencher system was performed by absorbance, steady-state and time-resolved fluorescent spectroscopy. First, absence of ground-state interaction between the photocatalyst and BnNH₂/BnOH is verified by the absorption spectra before and after addition of the quencher.

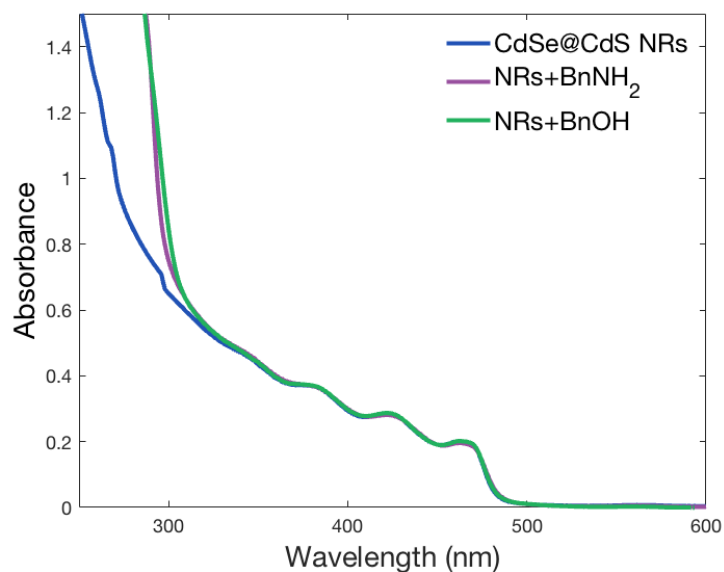


Figure S2. Absorption spectra of the bare NRs/quencher system acquired during Stern-Volmer analysis.

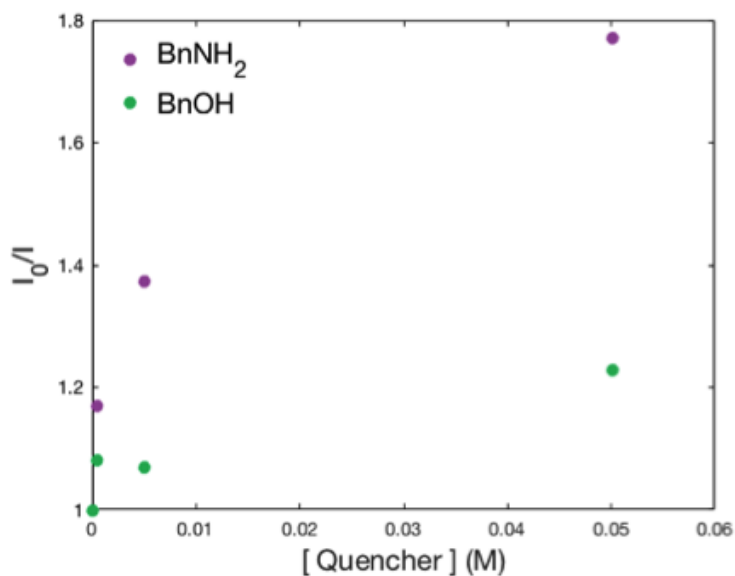


Figure S3. Stern-Volmer analysis of the bare NRs / quencher system, performed by steady-state fluorescent spectroscopy.

The plot in Figure S3 is obtained by monitoring the emission intensity maximum of a solution of bare NRs in H₂O:ACN (60:40), that is titrated with increasing amount of BnNH₂/BnOH, and calculated according to the following formula:

$$\frac{I_0}{I} = 1 + \tau_0 k_Q [Q] \text{ or } \frac{\tau_0}{\tau} = 1 + \tau_0 k_Q [Q]$$

where I_0 (τ_0) and I (τ) are the emission intensity maxima (excited-state lifetime) of bare NRs without and with increasing amount of quencher in solution, respectively, k_Q the quenching-constant and $[Q]$ the quencher concentration, i.e. $[BnNH_2]$ or $[BnOH]$, in solution. On the other hand, Figure S4 displays the Stern-Volmer analysis performed by monitoring the long-lived component of the multi-exponential excited-state lifetime decay:

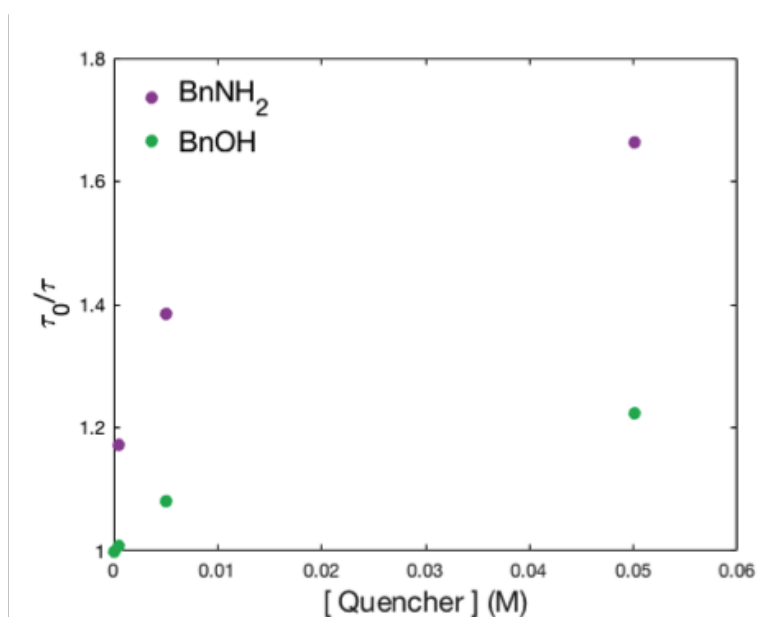


Figure S4. Stern-Volmer analysis of the bare NRs/quencher system performed by time-resolved fluorescent spectroscopy.

4 HYDROGEN PRODUCTION MEASUREMENTS

4.1 Experimental setup and methodology

Rods solutions were moved to ultrapure water by MUA ligand exchange as close as possible to starting a new measurement, usually less than one hour before the cell was first purged. Samples were diluted using ultrapure water, after which desired amounts of BnNH_2 or BnOH were added to make 10mL solutions. The gas tight reaction cells (Figure S5) were closed and connected to a 10mL/min argon line (filtered 99.999% purity) and an Agilent 7890A Series gas chromatograph with a thermal conductivity detector (GC-TCD). The cell on the right has an inlet port that enables furfure injections of BnNH_2 , or to withdraw sample time aliquots. Gas was continually flowed through the cell in the dark while the solution was stirred and gas samples were automatically taken every 5-10 minutes for measurement to monitor the purging process.

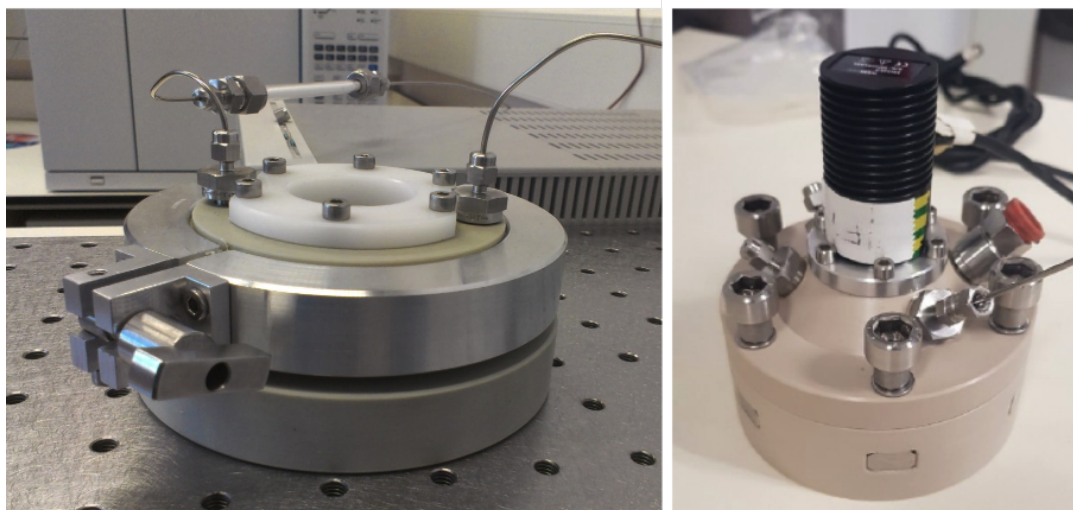


Figure S5. Photograph of the two types of gas-tight reaction cells (GC seen in the background on the left).

In a typical monochromatic excitation experiment a Thorlabs Royal Blue (455nm) high-power LED was switched on to illuminate the sample once the cell was fully purged. The photon flux was calculated by measuring the LED power (which was adjusted to a desired value and measured using a Thorlabs Digital Optical Meter – PM206) assuming all photons had the same wavelength of 455nm ($4.366 \cdot 10^{-19} \text{ J photons}^{-1}$). In this adjustment of the power we accounted for the irradiated area over the sample, as well as for the absorption of the reaction cell window and other minor losses in the setup. The LED power used during this work was 50 [mW], thus the photon flux (amount of photons per second) is $1.15 \cdot 10^{17} \text{ photons s}^{-1}$.

4.2 Calibration of the Gas Chromatograph

The hydrogen production rate generated by each sample was determined based on the area of the hydrogen gas peak, adjusted from $\mu\text{V}/\text{min}$ (as reported by the TCD) directly to the number of hydrogen molecules produced per min or in units of $\mu\text{L}_{\text{H}_2}/\text{min}$, via calibration. Calibration was performed using an electrolysis unit, built into a calibration cell that is identical to the sample cell, except that it has two nickel electrodes which can be connected to an external power supply. This method of calibration offers three distinct advantages over traditional calibration methodologies with a standard gas sample: (1) a calibration curve can be easily made with numerous points; (2) accurate calibration can be made even for extremely low amounts of hydrogen; and (3) the calibration precisely mimics the experimental conditions and thus is as accurate as can be.

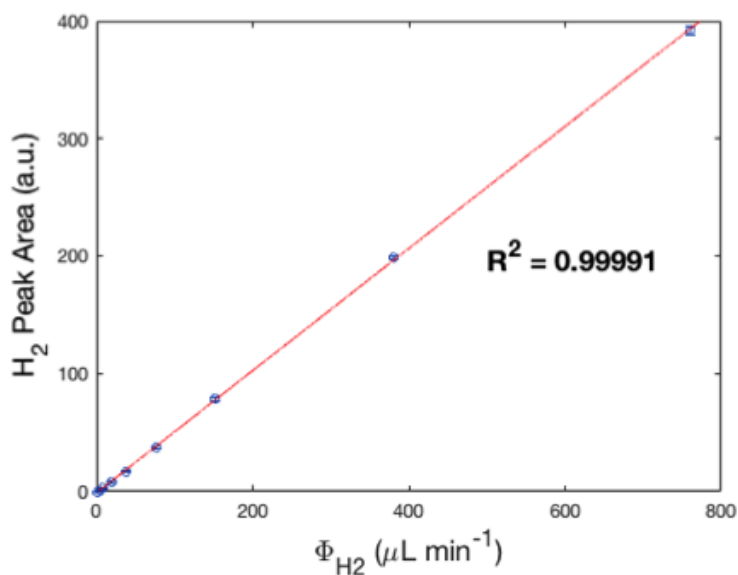


Figure S6. Calibration curve obtained for water electrolysis in the photoreactor cell, correlating detected H_2 flux to the peak area calculated with a Chem-Station software.

4.3 Determination of Photocatalyst Mass

In order to evaluate the hydrogen production rate per rod, or mass of catalyst, we evaluated the number of rods in a typical sample solution. CdSe@CdS-Pt photocatalyst quantification was carried out consistently following recent publications from our group[5,6]. In particular, we evaluated the number of rods in a typical sample solution by a calibration that correlates the rods absorption to Cd concentration in the solution as determined with ICP. The concentration [C] of a typical sample was around 0.49 [mM].

Using the dimensions of a typical sample and the literature value for CdS bulk density one can calculate the mass per a single rod:

$$\begin{aligned}l_{NR} &= 43.7 \text{ [nm]}, d_{NR} = 4.5 \text{ [nm]}, \rho_{CdS} = 4.824 \text{ [g cm}^{-3}\text{]} \\V_{NR} &= \pi \cdot 2.25^2 \text{ [nm}^2\text{]} \cdot 43.7 \text{ [nm]} = 6.95 \cdot 10^{-19} \text{ [cm}^3\text{]} \\m_{NR} &= 4.824 \text{ [g cm}^{-3}\text{]} \cdot 6.95 \cdot 10^{-19} \text{ [cm}^3\text{]} = 3.35 \cdot 10^{-18} \text{ [g]}\end{aligned}$$

For a sample with concentration of 0.49 [mM] the mass of CdS in solution is calculated to be:

$$\begin{aligned}M_w &= M_{w,Cd} + M_{w,S} = 144.475 \text{ [g mol}^{-1}\text{]} \\m &= C \cdot V \cdot M_w = 0.493 \text{ [mol L}^{-1}\text{]} \cdot 0.096 \text{ [L]} \cdot 144.475 \text{ [g mol}^{-1}\text{]} = 6.79 \cdot 10^{-4} \text{ [g]}\end{aligned}$$

Yielding a number of NRs per sample:

$$\#_{NRs} = \frac{m_{sample}}{m_{NR}} = \frac{6.79 \cdot 10^{-4} \text{ [g]}}{3.35 \cdot 10^{-18} \text{ [g]}} = 2.02 \cdot 10^{14}$$

Calculating the overall mass of the sample requires the addition of the Pt component (the previous calculations were for CdS rods only). Again we use the typical dimensions of an average Pt tip as obtained from the TEM, and calculate the mass from the volume and bulk density.

$$\begin{aligned}d_{QD,tip} &= 3 \text{ [nm]}, \rho_{Pt} = 21.45 \text{ [g cm}^{-3}\text{]} \\V_{QD,tip} &= \frac{4}{3} \cdot \pi \cdot (3 \cdot 10^{-7})^3 \text{ [cm}^3\text{]} = 1.41 \cdot 10^{-20} \text{ [cm}^3\text{]} \\m_{QD,tip} &= 21.45 \text{ [g cm}^{-3}\text{]} \cdot 1.41 \cdot 10^{-20} \text{ [cm}^3\text{]} = 3.03 \cdot 10^{-19} \text{ [g]} \\m_{PhotoCat} &= m_{NR} + m_{QD,tip} = 3.66 \cdot 10^{-18} \text{ [g]}\end{aligned}$$

The total mass of the sample will thus be:

$$m_{tot} = m_{PhotoCat} \cdot \#_{NRs} = 7.4 \cdot 10^{-4} \text{ [g]} = \mathbf{0.74 \text{ [mg]}}$$

4.4 Calculating Quantum Efficiency for Hydrogen Production

The GC measurement results with an area for the H₂ peak, which is converted using the calibration to H₂ production flow rate [H₂/min]. For example, with BnNH₂ oxidation that is presented in Figure 2B, at 50mW of excitation power, we obtained a flow of 41.07 H₂ [$\mu\text{L min}^{-1}$], which is equivalent to $1.68 \cdot 10^{16}$ [H₂ molecules s⁻¹].

Since in the course of this work the sample concentration was not fully adjusted to be near 100% absorption (per the reaction cell depth), the QE was calculated with regard to the absorbed rather than incident photons. Each hydrogen molecule production requires two electrons, and therefore two photons. Thus the quantum efficiency of the sample is defined as $QE_{PTH} = 2N_{H_2}/(N_{hv} \cdot OD)$, with $OD = 1 - 10^{-A}$. Experiments are typically performed with $OD = 0.8$.

$$QE_{PTH} = \frac{2 \cdot 1.68 \cdot 10^{16} \left[\frac{H_2}{sec} \right]}{1.15 \cdot 10^{17} \cdot 0.8 \left[\frac{Photons}{sec} \right]} = \mathbf{0.37}$$

Thus when illumination with a power of 50mW at 455nm resulted with hydrogen production rate of 41 H₂ [$\mu\text{L min}^{-1}$], we were operating at 37% photons to hydrogen conversion efficiency.

4.5 Calculating TOF

Photocatalyst activity is evaluated in terms of Turn Over Frequency (TOF), i.e. the ratio between the generated H₂ molecules flux, N_{H_2} , and the total number of NRs present in the sample, $\#_{NRs}$:

$$TOF = \frac{N_{H_2}}{\#_{NRs}} \left[\frac{H_2 \text{ molecules}}{\#_{NRs} \cdot h} \right] = \frac{1.68 \cdot 10^{16} \left[\frac{H_2}{sec} \right] \cdot 3600 \left[\frac{sec}{h} \right]}{2 \cdot 10^{14}} = 302,400 \left[\frac{H_2 \text{ molecules}}{\#_{NRs} \cdot h} \right]$$

Hence with a hydrogen production rate of $1.68 \cdot 10^{16}$ [$\frac{H_2}{sec}$], generated from only $2 \cdot 10^{14}$ rods, we are looking at about 84 hydrogen molecules that are being generated on a single rod every second, and a turn over number of

$$TOF \sim \mathbf{300,000} \left[\frac{H_2 \text{ molecules}}{rod \cdot hr} \right].$$

The total mass of the sample was calculated to be ~ 0.74 mg, so that the peak of H₂ production coupled with BnNH₂ oxidation under excitation at 455nm per unit of mass of catalyst per hour is:

$$Q_{H_2} = \frac{2.8 \cdot 10^{-8} \left[\frac{H_2 \text{ mol}}{sec} \right] \cdot 3600 \left[\frac{sec}{h} \right]}{0.00074 [g]} = 0.136 \left[\frac{mol H_2}{g \cdot h} \right]$$

$$Q_{H_2} = \mathbf{0.136} \left[\frac{mmol H_2}{g \cdot h} \right]$$

4.6 Calculation of Fraction of Light Absorbed.

While η_{PTH} evaluation is straightforward when using monochromatic light sources, experiments using simulated solar sunlight consider photon fluxes according to the following formula:

$$J_{ph} = \int_{\lambda_1}^{\lambda_2} \frac{J_{AM1.5G,e,\lambda}}{E_\lambda} \cdot \eta_{abs,\lambda} d\lambda \cdot A$$

where J_i denote photon -suffix 'ph'- or energy -suffix 'e'- fluxes, E the photon energy, A the irradiated area and $\eta_{abs,\lambda}$ the fraction of light absorbed by the photocatalyst, or light harvesting efficiency, at each wavelength – suffix λ . The latter quantity is determined by the Beer-Lambert-Bouguer law for liquid solutions:

$$\eta_{abs,\lambda} = 1 - 10^{-A_\lambda} = 1 - 10^{-\epsilon_\lambda c l}$$

while the integral is evaluated in a spectral range specified by experimental conditions. Typically, solar-simulation is fractioned by a 400nm long-pass filter and by the photocatalyst valence-band energy, that impose photon absorption only if $E_\lambda \geq 2.48eV$ ($\lambda \leq 500nm$). Furthermore, we also take into account optical losses occurring in between radiation source and solution surface by dividing J_{ph} for a scaling factor. Attenuation losses are measured using a Thorlabs PM206 Digital Optical Meter equipped with a 0.19 – 25 μm thermal sensor at the solution surface. Overall, we estimate J_{ph} to be $4.82 \cdot 10^{15} ph.s^{-1}$ (corresponding to a light intensity of 0.1 sun) for the experiment using the solar-simulator represented in Fig.4, compared to $1.15 \cdot 10^{17} photons s^{-1}$ provided by the Thorlabs High-Power LED M455L3.

4.7 Control Experiments

Control experiments were performed in a H₂O:ACN (60/40) mixture, in absence of (1) CdSe@CdS-Pt photocatalysts, (2) hole scavenger, or (3) light. The residual activity observed in absence of hole scavengers can be ascribed to the combined H₂ generation and photo-oxidation of the mercaptoundecanoic-acid ligands stabilizing the NRs, and even oxidation of the CdS itself. Such detrimental process unsurprisingly results in the rapid degradation of the colloidal system, as demonstrated by the concomitant decrease in activity.

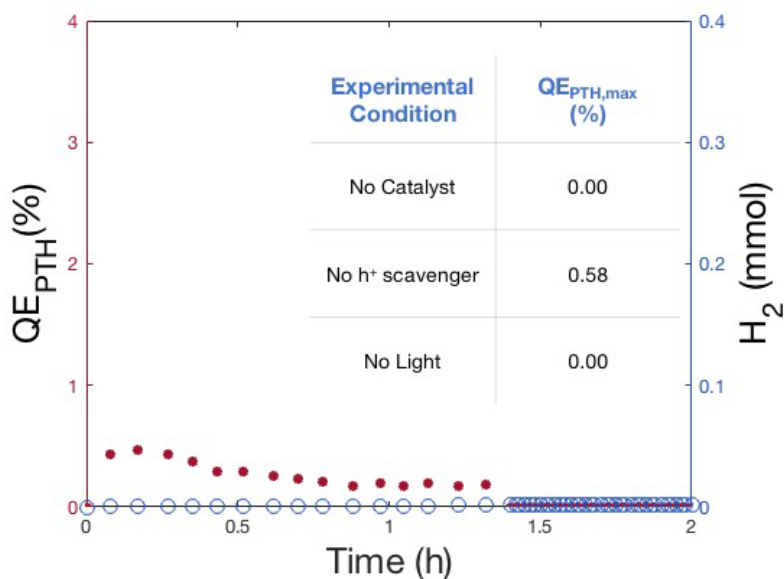


Figure S7. Control experiments performed in a H₂O:ACN (60/40) mixture, in absence of (1) CdSe@CdS-Pt photocatalysts, (2) hole scavenger, and (3) light.

5 SOLAR-TO-CHEMICAL ENERGY CONVERSION CALCULATION

In order to calculate the fraction of solar chemical potential stored in chemical bonds formed after the photosynthetic reaction, we consider the solar-to-chemical (STC) efficiency:

$$STC = \frac{J_{rxn} \cdot \mu_{rxn}}{P_{AM1.5G} \cdot A} \cdot 100\%$$

where J_{rxn} is the chemical reaction rate, μ_{rxn} the chemical potential associated to the reaction realized and $P_{AM1.5G}$ the total incoming power. Under conditions of constant temperature and pressure, the chemical potential is the partial molar Gibbs free energy (ΔG).

Considering CdSe@CdS-Pt photocatalyst as a closed-circuit photoelectrochemical cell, we can define the chemical potential of the reaction as:

$$\mu_{rxn} = -n \cdot \mathcal{F} \cdot E^0$$

with n representing the number of electrons involved in the reaction, \mathcal{F} the Faraday constant and E^0 the cell potential, which is in turn expressed by the equation $E^0 = E_{cathode}^0 - E_{anode}^0$.

For the overall water splitting reaction:

$$\begin{aligned} 2H^+ + 2e^- &\rightarrow H_2, & E_{cathode}^0 &= -0.414 [V] \\ H_2O &\rightarrow \frac{1}{2}O_2 + 2H^+ + 2e^-, & E_{anode}^0 &= 0.816 [V] \\ \mu_{H^+/OH^-} &= -2 \cdot 96,485 \left[\frac{KJ}{V \cdot mol} \right] \cdot \{-0.414 - (0.816)\}[V] = \mathbf{237.1 [KJ mol^{-1}]} \end{aligned}$$

In our case, reduction of water occurs simultaneously with oxidation of benzylamine to the corresponding imine, i.e. benzylidenebenzylamine (*BI*). Among the body of discording values for the oxidation potential of $BnNH_2$ [7–9], we adopted the one from Wang et al.[10], owing to the similar solvent used for cyclic voltammetry.

$$\begin{aligned} 2H^+ + 2e^- &\rightarrow H_2, & E_{cathode}^0 &= -0.414 [V] \\ 2BnNH_2 &\rightarrow BI + NH_4^+ + H^+ + 2e^-, & E_{anode}^0 &= 1.324 [V] \\ \mu_{H^+/BnNH_2} &= -2 \cdot 96,485 \left[\frac{KJ}{V \cdot mol} \right] \cdot \{-0.414 - (1.324)\}[V] = \mathbf{335.4 [KJ mol^{-1}]} \end{aligned}$$

Thus, according to the definition from Osterloh[11], as long as $E^0 < 0 V$, hence $\mu_{rxn} > 0 J mol^{-1}$, we have an endothermic reaction, i.e. a photosynthetic reaction. On the contrary, when $E^0 > 0 V$, $\mu_{rxn} < 0 J mol^{-1}$, therefore the reaction is exothermic and conventionally defined as photocatalytic.

6 GAS-CHROMATOGRAPH MASS SPECTROSCOPY

GC-MS data was collected with a Hewlett-Packard 5971 spectrometer with GC injection and EI ionisation at 70 eV coupled with an Agilent Technologies MSD1100 single-quadrupole mass spectrometer, reported as: m/z (rel. intensity). The results obtained from GC-MS analysis of products from the combined H_2 generation and $BnNH_2$ oxidation are presented in the main text in figure 5. The GC-MS analysis of products from the combined H_2 generation and $BnOH$ oxidation are presented here in Figure S7.

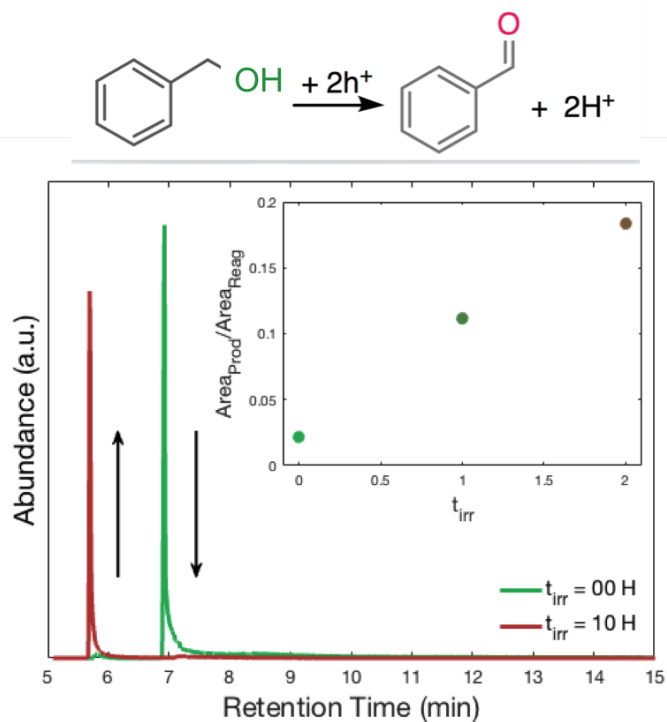


Figure S8. GC-MS analysis of products from the combined H_2 generation and $BnOH$ oxidation, displaying the progressive $BnOH$ consumption (green-curve) and $BnCHO$ (red-curve) production.

References

- [1] L. Carbone, C. Nobile, M. De Giorgi, F. Della Sala, G. Morello, P. Pompa, M. Hych, E. Snoeck, A. Fiore, I.R. Franchini, M. Nadasan, A.F. Silvestre, L. Chiodo, S. Kudera, R. Cingolani, R. Krahne, L. Manna, Synthesis and Micrometer-Scale Assembly of Colloidal CdSe/CdS Nanorods Prepared by a Seeded Growth Approach, *Nano Lett.* 7 (2007) 2942–2950.
- [2] D. V. Talapin, J.H. Nelson, E. V. Shevchenko, S. Aloni, B. Sadtler, A.P. Alivisatos, Seeded Growth of Highly Luminescent CdSe/CdS Nanoheterostructures with Rod and Tetrapod Morphologies, *Nano Lett.* 7 (2007) 2951–2959.
- [3] T. Mokari, E. Rothenberg, I. Popov, R. Costi, U. Banin, Selective Growth of Metal Tips onto Semiconductor Quantum Rods and Tetrapods, *Science.* 304 (2004).
- [4] C. Würth, M. Grabolle, J. Pauli, M. Spieles, U. Resch-Genger, Relative and absolute determination of fluorescence quantum yields of transparent samples, *Nat. Protoc.* 8 (2013) 1535–1550.
- [5] P. Kalisman, Y. Nakibli, L. Amirav, Perfect photon-to-hydrogen conversion efficiency, *Nano Lett.* 16 (2016) 1776–1781.
- [6] Y. Nakibli, L. Amirav, Selective Growth of Ni Tips on Nanorod Photocatalysts, *Chem. Mater.* 28 (2016) 4524–4527.
- [7] K. Ohkubo, T. Nanjo, S. Fukuzumi, Photocatalytic Electron-Transfer Oxidation of Triphenylphosphine and Benzylamine with Molecular Oxygen via Formation of Radical Cations and Superoxide Ion, *Bull. Chem. Soc. Jpn.* 79 (2006) 1489–1500.
- [8] T. Łuczak, Electrochemical behaviour of benzylamine, 2-phenylethylamine and 4-hydroxyphenylethylamine at gold. A comparative study, *J. Appl. Electrochem.* 38 (2007) 43–50.
- [9] A. Thirumoorthi, K.P. Elango, Solvent and substituent effects on the electrochemical oxidation of substituted benzylamines in 2-methylpropan-2-ol/water medium, *Int. J. Chem. Kinet.* 39 (2007) 371–377.
- [10] Z.J. Wang, K. Garth, S. Ghasimi, K. Landfester, K.A.I. Zhang, Conjugated Microporous Poly(Benzochalcogenadiazole)s for Photocatalytic Oxidative Coupling of Amines under Visible Light, *ChemSusChem.* 8 (2015) 3459–3464.
- [11] F.E. Osterloh, Photocatalysis versus Photosynthesis: A Sensitivity Analysis of Devices for Solar Energy Conversion and Chemical Transformations, *ACS Energy Lett.* 2 (2017) 445–453.